Chapter 16

High Thermal Conductivity Ceramics and Their Composites for Thermal Management of Integrated Electronic Packaging

Hyo Tae Kim

Additional information is available at the end of the chapter

http://dx.doi.org/10.5772/intechopen.75798

Abstract

Recently, ceramic substrates have been of great interest for use in light emitting diode (LED) packaging materials because of their excellent heat transfer capability. The thermal conductivities of ceramic-based substrates are usually one or two orders of magnitude higher than those of conventional epoxy-based substrates. The demand for ceramic substrates with high mechanical strength and thermal conductivity is also growing due to their use in thin and high-power device packaging substrates. Examples are direct bonded copper or aluminum or direct plated copper substrates for insulated gate bipolar transistors; thin and robust ceramic packages for image sensor modules that are used in mobile smart phones; ceramic packages for miniaturized chip-type supercapacitors; and high-power LED packages. This chapter will cover the development and application of ceramics and ceramic composites with high thermal conductivity for the thermal management of integrated electronic packaging substrates such as high-power LED packaging, power device packaging, etc.

Keywords: thermal conductivity, ceramics, composites, electronic, packaging

1. Introduction

Ceramic materials with high thermal conductivity are of great interest in the thermal management of integrated electronic device packaging such as high-power light emitting devices (LEDs), power semiconductor modules, micro and nano fluidics, thermoelectrics, solar cells, and wireless communication devices. These electronic devices and packages generate more heat than before as the system design goes into more integrated, miniaturized, and increasing

data communication due to the multifunctional requirement in wireless communication and the Internet of things (IOT) environment. Moreover, a global movement for a clean environment has shifted the public interest from conventional cars with combustion engines to electric vehicles (EVs) and hybrid electric vehicles (HEVs), thus drastically increasing the use of integrated power modules with increased powers and operation frequencies. In this regard, the development of high thermal conductivity ceramics for packaging substrate and filler materials for composites is of great importance. This chapter briefly examines recent trends, development, and technical issues of selected high thermal conductivity ceramic materials and their composites.

2. High thermal conductivity ceramics and their composites

2.1. Aluminum nitride (AlN) base ceramics and composites

2.1.1. AlN ceramics with sintering additives

Aluminum nitride (AlN) has a highly covalent bonded wurtzite structure with a high thermal conductivity and a low thermal expansion coefficient (CTE) of 4.5 ppm/°C that matches well with silicon devices. Typical thermal conductivity of AlN is 140–180 W/mK but varies in the range 18–285 W/mK in polycrystalline AlN ceramics depending on the process condition, purity of starting materials, and microstructures [1]. AlN is stable at 700–1000°C in an oxygen atmosphere. It also has excellent dielectric properties: low dielectric constant (ε_r) = 9 and low loss (tan δ) = 0.0003 at 1 MHz. With these outstanding physical and thermal properties, AlN ceramic is frequently selected as a candidate material for insulating substrate (direct band gap energy ~6.015 eV) for power electronics device and package. However, sintering of AlN with high density for effective heat transfer and high mechanical strength is challenging due to its highly covalent and low diffusive nature that requires very high sintering temperatures over 1900°C in a reducing atmosphere with applied pressure even though it is stable near 1000°C in air. Also, degradation of thermal conductivity due to oxygen inclusion is another confronting issue in high thermal conductivity AlN substrate fabrication.

Many works to promote the densification of AlN ceramic bodies using different kinds of sintering additives such as CeO, Sm_2O_3, Y_2O_3, CaO, $CaZrO_3$, and their multiple co-additions have been investigated [2–5]. Some of the recent results showing the thermal conductivities obtained in polycrystalline bodies are 90–156 W/mK as summarized in **Table 1**, which is far below the theoretical value and has a wide span from each other. Ceria (CeO) doped AlN exhibited a stiff increase in thermal conductivity and decent increase in mechanical strength with a small amount of addition (~1.5 wt%), compared to the yttria (Y_2O_3) addition [2]. High energy sintering method like spark plasma sintering (SPS) was applied [3, 4] as well as conventional solid state reaction (SSR) method [2] for effective low temperature densification process. The two-step sintering technique was also conducted using different temperatures to minimize grain growth and purification of AlN grains [5] (**Figure 1**).

Chemical composition	Sintering additives	Thermal conductivity (W/mK)	Mechanical properties	Sintering temp/ method	Ref.
AlN	1.5 wt% CeO	156	72.46 kg/mm^2	1900°C/SSR	[2]
AlN	2 wt% Sm_2O_3	120	—	1700°C/SPS	[3]
AlN	Y_2O_3-CaO-B	90	—	1650°C/SPS	[4]
AlN	$CaZrO_3$-Y_2O_3	156	560 MPa	1550°C/Two-step	[5]

Table 1. Physical properties of AlN ceramics with the addition of sintering additives and densification methods.

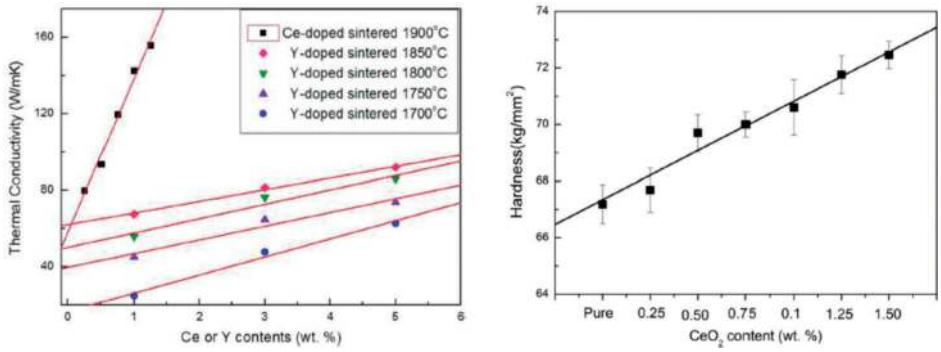

Figure 1. Effect of Ce and Y doping on the thermal conductivity and hardness of AlN ceramics [2].

2.1.2. AlN composites with GNP/GNS/rGO: electrically conducting

Carbon based nanostructured materials such as graphene nanoplatelets (GNP) or nanosheets (GNS) were added to AlN matrix to improve physical properties (**Table 2**). The electrical conductivity was increased with the addition of multilayer graphene as expected but the thermal conductivity was decreased with the addition in both in-plane and through-plane direction, which is adverse to other ceramic/graphene composites data. This sharp decline of thermal conductivity in both directions seems attributed to the large thermal resistance at the thin interaction zone existing in the interface between AlN and GNP [6]. The high directionality in the in-plane and through-plane of AlN/GNP composites, 74 W/mK for in-plane and 37 W/mK for through-plane, is ascribed to the thermal contact resistance existing in both phase interfaces that are severe in the perpendicular heat transfer direction of graphene nanoplatelets [7]. This strong directionality in heat transfer, thermal conductivity, can be easily found in the boron nitride (BN)/polymer composite system, in which 2D morphology BN filler materials are used [9–16]. In case of reduced graphene oxide (rGO) added AlN, the thermal conductivity decreased sharply from 92.5 to 37.4 W/mK when 2 wt% of rGO was added, though there are minor increases in flexural strength and fracture toughness at ≤1 wt% of rGO, which is due to the low crystallinity, high vacancy defects in rGO, and increased interfacial thermal resistance [8]. The declining thermal conductivity behaviors of AlN composites with these three carbon based 2D fillers exhibited almost similar results as GNP, GNS, and rGO basically

Chemical composition	Additives	Thermal conductivity (W/mK)	Mechanical properties	Sintering temp./ method	Ref.
AlN-2.9 wt%Y_2O_3-GNP~10 vol%	GNP 0.1 vol%	74 (in-plane) 37 (through-plane)	—	1700-1750/SPS	[6]
AlN-2wt%Y_2O_3	GNS 1.49 vol%	—	FS = 441 MPa FT = 4.09 MPam$^{1/2}$	1850/hot press	[7]
AlN	rGO 1 wt%	92.5 - > 37.4 (2 wt%)	FS = 375 MPa	1550/SPS	[8]

FS: Flexural strength; FT: Fracture toughness; SPS: Spark plasma sintering

Table 2. Physical properties of AlN with carbon nanomaterials addition.

had the same morphology and physical properties. High thermal conductivity materials with high directionality in heat transfer can be used in specific directional heat dissipation applications as thermal interface materials (TIM) (**Figures 2** and **3**).

2.1.3. Si_3N_4 base ceramics

Silicon nitride (Si_3N_4) ceramics has been drawing a lot of interest as a high thermal conductivity dielectric material used in insulated metal substrate (IMS) for power electronic circuit modules. Si_3N_4 have several benefits: high mechanical properties (flexural strength >800 MPa, Vickers' hardness >10 GPa), high electrical resistivity, and excellent thermal properties with thermal resistance, high thermal conductivity 70–180 W/mK. However, in reality, fabrication of Si_3N_4 with high thermal conductivity and high mechanical strength is not easy due to difficulties in densification and morphological control in microstructure. Typical approaches to get such a high performance Si_3N_4 are: (i) using raw materials with low oxygen to remove Si vacancies that cause phonon scattering, (ii) fabrication of Si_3N_4 ceramics with textured microstructure to utilize thermal anisotropy in Si_3N_4 crystals, (iii) using non-oxide sintering additives with low oxygen content to avoid oxygen content from the oxide phase, and (iv) selecting optimal additives that can minimize the Si vacancies [9]. Some of selected results based on these approaches

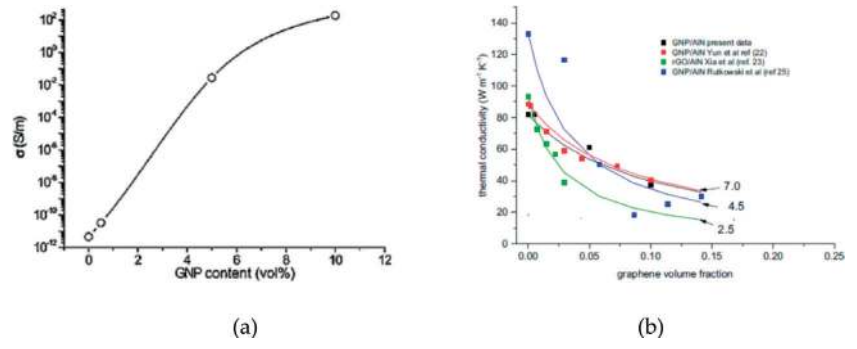

Figure 2. AC electric conductivity (a) and thermal conductivity data (b) with GNP content in the AlN composites [6].

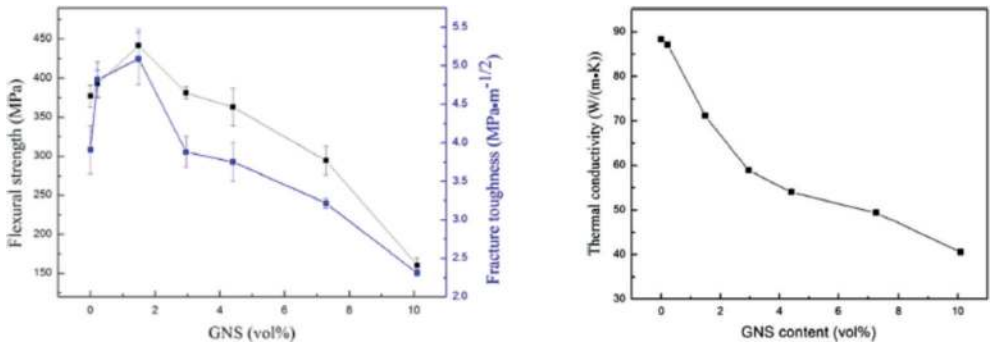

Figure 3. Fracture toughness and flexural strength of AlN/GNS composites [7].

are summarized in **Table 4**. When non-oxide additives like YF_3 was added to Si_3N_4 with MgO instead of Y_2O_3, the mechanical strength and thermal conductivities were improved from 40 to 52; it was further increased to 75 W/mK after the annealing treatment at 1850°C. However, Vickers' hardness was decreased slightly due to larger particle sizes than with the Y_2O_3 addition [9]. The thermal conductivity of Si_3N_4 increased up to 100 W/mK when Yb_2O_3/SiO_2 was added and the dielectric loss was decreased from 11.5×10^{-4} to 1.4×10^{-4} (2 GHz) by adjusting the ratio from 0.33 to 1.3 [10]. The influence of nitration and sintering conditions on the mechanical and thermal properties of the sintered reaction bonded Si_3N_4 (SRBSN) with Y_2O_3-MgO additives, and the coarsening of grain size and aspect ratio decreased the hardness and fracture toughness while increasing the thermal conductivity. Vickers' hardness of 17.32 GPa, fracture toughness of 8.36 MPa·$m^{1/2}$, and thermal conductivity of 98.52 W/m·K were obtained by adjusting nitration and gas pressure sintering (GPS) [11]. A comparative study of the effects of oxide and non-oxide additives on the microstructure, lattice oxygen content, and thermal conductivity of Si_3N_4 ceramic was investigated. Non-oxide additives such as $MgSiN_2$, YF_3, YbF_3 induced a decrease in the amount of secondary phases and lattice oxygen contents, thus increasing thermal conductivity from 65 to 101.5 W/mK, while the flexural strength was not affected significantly [12].

2.1.4. AlN-BN base composites: electrically insulating

Boron nitride (BN) was introduced in the AlN matrix to realize low dielectric constant and moderate thermal conductivity [17]. Boron nitride (h-BN) has a hexagonal structure with good thermal shock resistance and high thermal conductivity together with directional preference in heat transfer, i.e., anisotropy in thermal conductivities at in-plane and through-plane of the substrate due to the 2D shape of the BN flake or BN nanosheet. The in-plane and through-plane thermal conductivities are about 300 and 30 W/mK, and the average apparent value is 33 W/mK. The h-BN has low dielectric constant and loss tangent, ε_r = 4–4.6, tan δ = 0.0012–0.0017 at 8.8 GHz, and dielectric strength at AC = 67–95 kV, which varies depending on the purity. BN has been used in many applications due to these excellent properties, for example, in microelectronic packaging especially in thermal management parts such as heat sinks and power electronic substrates, etc. The addition of BN to AlN also can improve chemical resistance and moisture resistance since the AlN can be hydrolyzed slowly in water (**Table 3**).

Chemical composition	Additives	Thermal conductivity (W/mK)	Sintering temp/method	Ref.
AlN–BN	Sm_2O_3-CaF_2	40–85	1800/SPS	[17]
AlN–BN(15%)	Y_2O_3	141	1800/SPS	[18]
AlN–BN	CaF_2	110	1850/hot-press	[19]
(Al-O-N)–BN		⊥14, //42.5	1900/hot-press	[20]

Table 3. Thermal conductivities of AlN–BN composites.

In the AlN–BN composites with 8 wt% Sm_2O_3-CaF_2 as sintering aid, the highest thermal conductivity of 85 W/mK and lowest loss tangent of 4×10^{-3} were achieved at the sintering temperature of 1800°C by the SPS method. The obtained thermal conductivity was lower than that of pure AlN because the platelet BN particles randomly distributed along the AlN matrix hinders direct contact of AlN so that phonon scattering is inhibited [17]. When yttrium oxide (Y_2O_3) from 3 to 8 wt% is added to the AlN–15%BN composites, the thermal conductivity was increased from 110 to 140 W/mK, which is attributed to the significant decrease in residual grain boundary phase containing yttrium by using SPS method [18]. The addition of CaF_2 and increasing temperature also improved the densification, thermal conductivity, and grain boundary purification at the AlN–BN system. As a result, high thermal conductivity of 110 W/mK was obtained when 3 wt% of CaF_2 was added and sintered at 1850°C [19]. In the aluminum oxynitride (γ-AlON)–BN system that was prepared by the self-propagating high-temperature synthesis (SHS) process, platelet shaped h-BN grains are re-oriented during the hot-pressing process resulting in the anisotropy of thermal conductivities. The thermal conductivity of (γ-AlON)–BN composites were 14 W/mK for through-plane direction of BN grains and 42.5 W/mK for in-plane direction which is perpendicular to the hot-pressing force [20] (**Figure 4**).

2.2. Polymer matrix composites with high thermal conductivity ceramic fillers

Polymer matrix composites for thermal management packaging are usually filled with high thermal conductivity ceramics such as AlN, h-BN, and carbon based fillers like carbon nano

Main element	Sintering additives	Thermal conductivity (W/mK)	Mechanical properties	Sintering condition	Ref.
Si_3N_4	YF_3, MgO	52–75	87 MPa/14.8 GPa	1750–1850°C/20 MPa	[9]
Si_3N_4	Yb_2O_3, SiO_2	46–100	—	1900°C/0.9 MPa	[10]
Si_3N_4	Y_2O_3, MgO	98.52	—/17.52 GPa	1950°C/GPS	[11]
Si_3N_4	MgO-Y_2O_3, $MgSiN_2$-Y_2O_3, $MgSiN_2$-YF_3, MgO-Yb_2O_3, $MgSiN_2$-Yb_2O_3, and $MgSiN_2$-YbF_3	101.5	862 MPa	1800°C/250 MPa	[12]

Table 4. Physical properties of Si_3N_4 ceramics with the addition of sintering additives and densification methods.

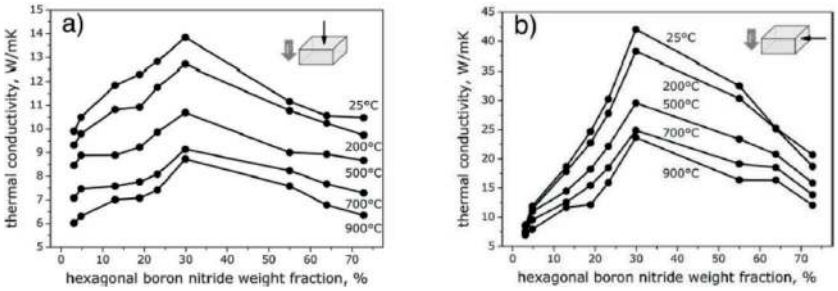

Figure 4. Compositional dependence of thermal conductivity of the composites in the (γ-AlON)–BN system determined in (a) perpendicular and (b) parallel to the pressing force [20].

fibers (CNTs), graphite or graphene nanosheets (GNSs), and reduced graphene oxide (rGO). Polymers with AlN and h-BN ceramic filler systems are mostly preferred for high thermal conductivity with electrically insulating heat transfer substrates or thermal interface materials (TIM) due to the high thermal conductivity, low dielectric constant and low loss characteristics of AlN and BN ceramics. On the other hand, carbon based fillers are preferred in TIMs where electrically conducting characteristics are allowed.

2.2.1. Polymer: BN composites

In the hexagonal-boron nitride (h-BN) filled polymer composites, the major issues to enhance heat transfer property are surface treatment of h-BN platelet particles to improve the dispersion of the filler particles in the polymer matrix; to lower the interface thermal resistance; and to increase the alignment of h-BN particles to the preferred orientation in order to achieve high directional thermal conductivity in composites. **Table 5** summarizes several technical efforts to enhance the heat transfer properties of polymer–BN composites [13–16, 21–24].

A combined technique that uses mechanical vibration and rotating magnetic field induced high degree of alignment of 10% filler loaded composite exhibited 74% improvement in thermal conductivity compared to the unaligned sample by the formation of conductive network and the reduction of the thermal boundary resistance. The reduction in the thermal boundary resistance between h-BN and bisphenol-A based resin was induced by a high degree of alignment of h-BN platelets via the combined process [13].

The effect of AC and DC electric fields on the anisotropically aligned microstructure in the h-BN filled silicone rubber composites was studied. It was found that the degree of re-orientation of h-BN was more effective under the AC than the DC field during the curing process of the h-BN-silicone composite (**Figure 5**), and the thermal conductivity of the e-field assisted curing composite was about 250% higher than that cured without *E*-field [14]. In a recent study, the largest total number of linear densely packed BN nanosheets (LDPBNs) was formed by applying AC field, and thickening of LDPBNs and narrowing of interparticle gaps were achieved by applying a switching DC field (**Figure 6**). As a result, the thermal conductivity was increased four times that of the composite without LDPBN structure [15].

Composition	BN %	Thermal conductivity (W/mK)	BN align method	Ref.
BN–epoxy	10–20	74% ↑	Mechanical and magnetic	[13]
BN–silicone	20	250% ↑	E-field(AC, DC)	[14]
BN–polysiloxane	15 vol%	400%↑	AC/switching DC	[15]
BN–PVA	27 vol%	1.63 W/mK ⊥/8.44 W/mK//	PVA solution infiltration	[16]
BN–polyurethane acrylate (PUA)	30 vol%	190%↑(in-plane) 72%↓(through-plane)	e-field (TiO_2-coated BN)	[21]
BN–PEN(poly(arylene ether nitride))	30 wt%	140%	Magnetic + mussel inspired co-modification (Fe_3O_4/PDA + KH550)	[22]
BN		3.49 W/mK(45.4%)	Silane coupling agents with different carbon chain	[23]
BN–PVA	50 vol%	1.1 W/mK ⊥/13 W/mK//	Mechanical exfoliation, compression	[24]

Table 5. Examples of thermal conductivities of polymer–BN composites.

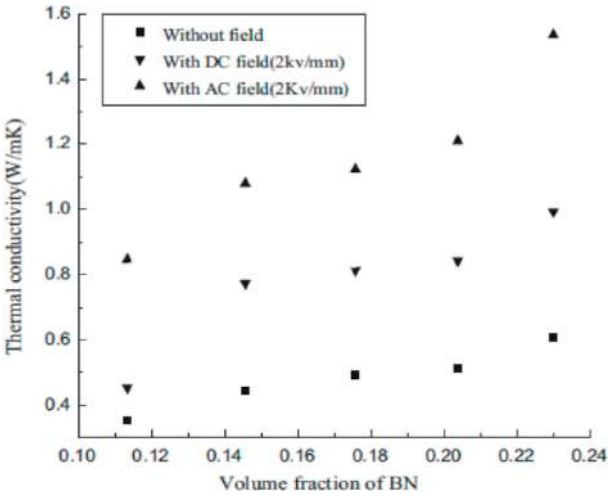

Figure 5. Thermal conductivity of BN/silicone composites at different volume fractions [14].

A flexible h-BN/poly(vinyl alcohol) composite tape was fabricated by the infiltration of poly(vinyl alcohol) (PVA) solution into the h-BN stack with vacuum filtration to reduce the gap between the h-BN particles and to increase the degree of alignment of h-BN platelets. The in-plane and through-plane thermal conductivities of h-BN/PVA composites thus obtained were 1.63 and 8.44 W/mK, respectively [16]. In the same h-BN/PVA system, the degree of the orientation of h-BN platelet particles can be improved by pressure assisted casting [24], where the degree of orientation of the h-BN particle can be observed by the characteristic peaks in the X-ray diffraction (XRD) data. In order to boost the alignment of h-BN particles, the coating of electric or magnetic field sensitive materials such as TiO_2 or Fe_3O_4 ceramics on to the h-BN

http://dx.doi.org/10.5772/intechopen.75798

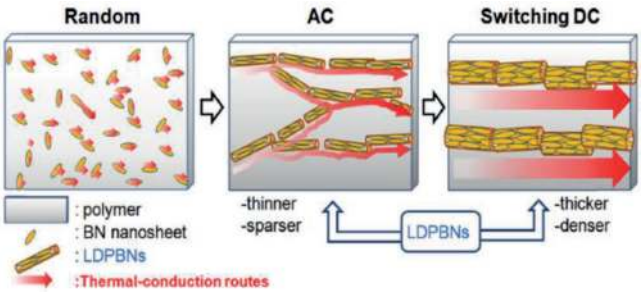

Figure 6. Schematic model of the generation of higher conduction routes through LDPBNs using various applications of electric fields [15].

particles are also explored to enhance the thermal conductivity [21, 23]. The h-BN particles coated with TiO_2 by the sol–gel process were aligned in a vertical direction to the applied field such that the through-plane thermal conductivity of h-BN/polyurethane acrylate (PUA) composite was increased by 190%, while the in-plane thermal conductivity of the composite was decreased by 72% compared to the untreated h-BN composite [21]. High dielectric constant and high thermal conductivity h-BN/poly(arylene ether nitrile) (PEN) composites were developed by magnetic alignment of h-BN through the coating of magnetic Fe_3O_4 particles together with an additional surface modification by polydopamine (PDA) and functional monomer KH550: (3-aminopropyl) triethoxy-silan). These surface modifications improved the dispersion of h-BN fillers in PEN matrix and the interfacial adhesion. In the BN/Fe_3O_4/PDA + KH550/PEN composite system, both dielectric constant and loss tangent were increased significantly with the amount of BN/Fe_3O_4/PDA + KH550, and the thermal conductivity was increased by 140% compared to the neat PEN film [22]. The enhancement of thermal conductivity in h-BN/epoxy composites through the surface modification of h-BN particles via silane coupling agents with different carbon chain has been investigated. The thermal conductivity of h-BN/epoxy composite was improved by 45.4% due to better dispersion of h-BN in epoxy resin than untreated h-BN, which attributed to the higher interfacial affinity of the composite obtained by using longer carbon chain of silane on the h-BN surface [23] (**Figures 7**, **8**, and **9**).

The effects of h-BN particle sizes, exfoliation of BN particles, and compression of h-BN/PVA composites on the thermal conductivity behavior were investigated [24]. **Figure 10(a)** shows that the thermal conductivity of h-BN/PVA composites was increased to almost two times when the as-received h-BN flakes are exfoliated into a thin h-BN nanosheet. Also, h-BN particles with smaller size exhibited a higher thermal conductivity in the h-BN/PVA composites, as shown in **Figure 10(b)**. Further increase in the thermal conductivity of h-BN/PVA composites were realized by uniaxial thermal compression after solution casting of h-BN/PVA composite film at 90°C which is above the glass transition temperature of the PVA polymer. **Figure 11** shows FE-SEM micrographs of the cross-sectional views of 30 vol% h-BN/PVA composites before (a) and after compression, which clearly show the h-BN particles alignment perpendicular to the pressing direction (b). The through (transverse)-plane and in-plane thermal conductivities measured by laser flash method are plotted together with theoretical modeling in **Figure 12**. Two models, arithmetic and Wiener models are used for the calculation of the two-phase composite system with the following equations.

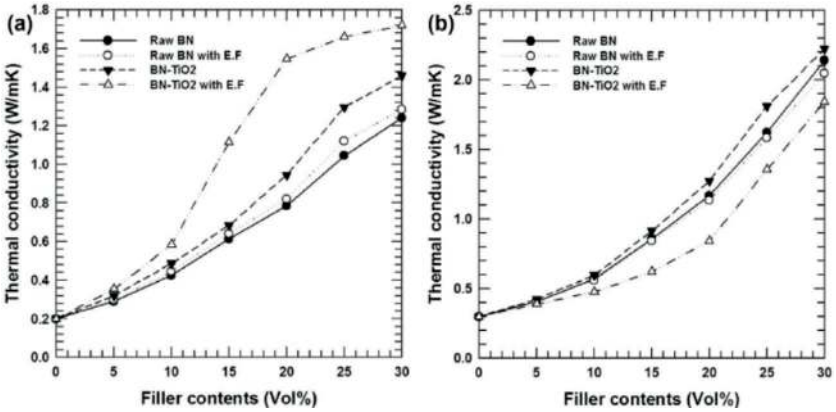

Figure 7. Thermal conductivity of h-BN/PUA composite and TiO_2 coated h-BN/PUA composite before and after electric field alignment: (a) through-plane and (b) in-plane thermal conductivity [21].

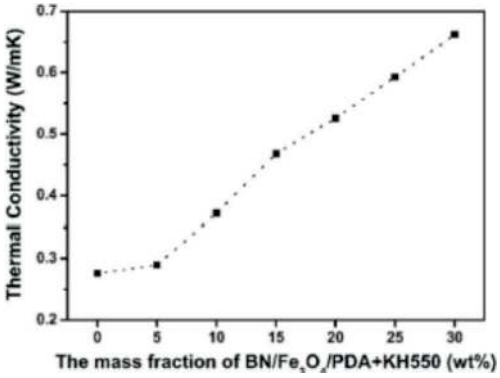

Figure 8. Thermal conductivities of neat PEN and BN/Fe_3O_4/PDA + KH550/PEN composite films with various amounts of filler loading content [22].

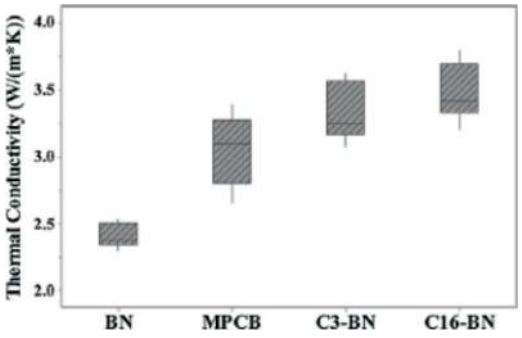

Figure 9. Thermal conductivities of h-BN/epoxy composites with untreated BN, MPCB (Al_2O_3/epoxy), silane (C3)/BN, and silane (C16)/BN [23].

http://dx.doi.org/10.5772/intechopen.75798

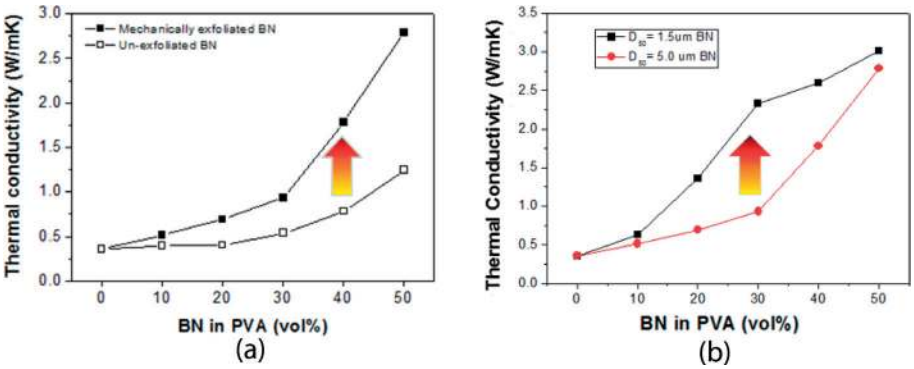

Figure 10. Effect of mechanical exfoliation (a) and h-BN particle sizes (b) on the through-plane thermal conductivities of h-BN/PVA composites [24].

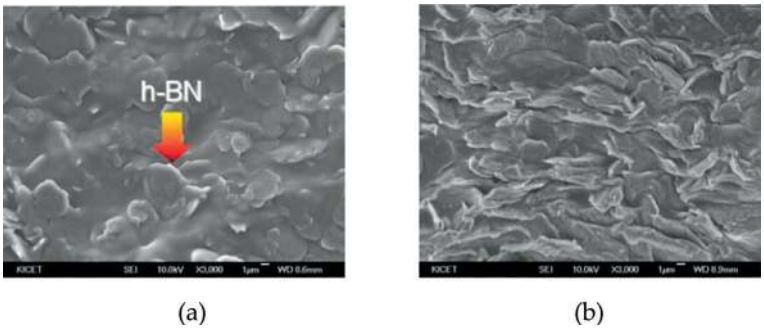

Figure 11. Cross-sectional views of 30 vol% h-BN/PVA composite films observed by FE-SEM: (a) uncompressed and (b) compressed [24].

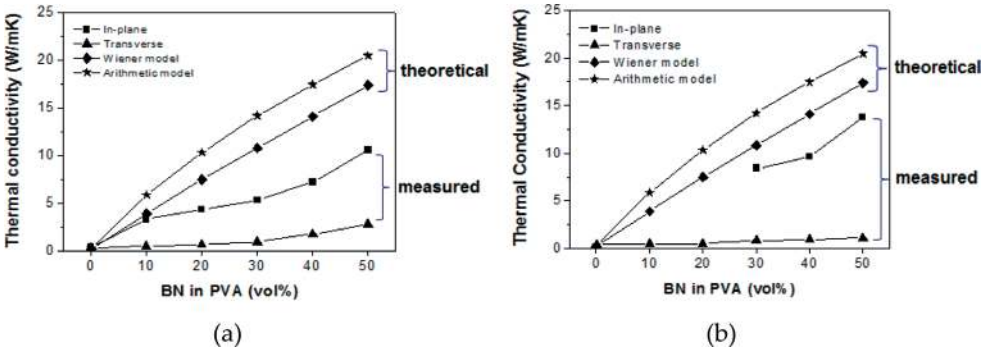

Figure 12. Effect of uniaxial compression on the transverse and in-plane mode thermal conductivities of h-BN/PVA composite films: (a) uncompressed and (b) compressed samples [24].

Arithmetic model:

$$\lambda = c\lambda_1 + (1 - c)\lambda_2 \tag{1}$$

where, c = proportion of component 1.

1–c = proportion of component 2

λ_1, λ_2 = thermal conductivity of component 1, 2.

Wiener model:

$$\lambda/\lambda_2 = \left(1 - c\left(\left(1 - \lambda_1/\lambda_2\right)/\left(1 + \alpha\,\lambda_1/\lambda_2\right)\right)\right)/\left(1 + \alpha c\left(\left(1 - \lambda_1/\lambda_2\right)/\left(1 + \alpha\,\lambda_1/\lambda_2\right)\right)\right) \tag{2}$$

where, $\alpha = 0.5$ for dispersion model, $\lambda_1 < \lambda_2$.

In this calculation, the thermal conductivity of PVA and h-BN was assigned as 0.2 and 33 W/mK, respectively. The in-plane, perpendicular to the compressing direction, thermal conductivities were 5 times higher than those of through-plane at the un-compressed samples, and had 10 times higher values at the compressed samples. The highest thermal conductivity obtained at 50 vol% h-BN loaded PVA composite was 13 W/mK in the in-plane mode, while that of through-plane mode was about 1.1 W/mK, which is lower than that the uncompressed sample [24]. The decrease in the through-plane mode thermal conductivity at the h-BN/PVA composites is due to the reduction in through-plane particle contact by the alignment of h-BN platelets parallel to the in-plane direction, which results in the increasing in-plane thermal conducting paths and decreasing through-plane thermal conducting paths. The Wiener model seems more close to the experimental data than the arithmetic model but the gap between these theoretical and experimental data is wide indicating that there still remain many factors that should be improved to reach an optimum condition in the fabrication of polymer/ceramic composites with high thermal conductivity.

In summary, several methods were explored to increase the thermal conductivity of h-BN/polymer composites. Examples are (i) surface modification of h-BN particles with functional organics to improve the affinity and dispersion of the h-BN/PVA solution, (ii) coating dielectric and ferrous ceramic materials on the h-BN particle to increase the alignment performance with the application of electric and magnetic field, (iii) exfoliation of h-BN flakes into thin h-BN nanosheets for better particle connection in a given filler loading, and (iv) mechanical compressing to promote particle alignment and inter-particle contact.

2.2.2. Polymer: AlN composites

Aluminum nitride (AlN) is a priority choice for filler material in high thermal conductivity polymer/ceramic composites since it has high thermal conductivity (320 W/mK, theoretical), good insulating (electrical resistivity > 10^{14} Ω·cm) characteristic, low dielectric constant (2.2–3.7 at 1 MHz), and low CTE (4.4 ppm/°C) which is close to silicon. In hot-pressed AlN/PMMA (polymethyl methacrylate) composites, thermal conductivity of 1.87 W/mK was obtained at 70 vol% AlN loaded composite which is about 10 times higher than the PMMA resin (0.18 W/mK) as shown in **Figure 13(a)**. The dielectric constant and loss of the composite were 4.4 (**Figure 13(b)**) and

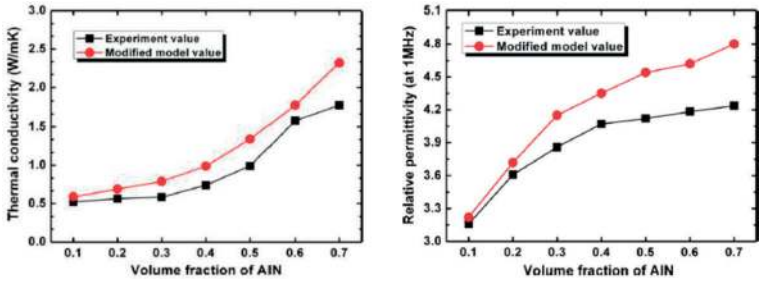

Figure 13. Experimental and calculated thermal conductivities data of PMMA/AlN composites with variation of AlN fillers [25].

0.017 at 1 MHz [25]. In the polypropylene (PP)/AlN composites with 3-D segregated structure made by mechanical grinding of PP and AlN mixture followed by hot-pressing at 190°C, core–shell structured PP/AlN composites were obtained. The comparative results of this 3D core–shell structure composite with conventional solution and melt mixed composites revealed that this mechanically ground composite with 10 vol% AlN showed 23% higher thermal conductivity than the others [26]. Thermal conductivity of aluminum nitride loaded poly(propylene glycol) (PPG) fluidic solution was also studied and the results have shown that the thermal conductivities of AlN/PPG fluids were dependent on the AlN solid loading and molecular weight of PPG [27].

In summary, in spite of efforts to increase thermal conductivity in polymer/ceramic composites, the thermal conductivities obtained in polymer matrix ceramic filled composites are still far below that of the fully ceramic base materials due to the low thermal conductivities in the polymer matrix which is limited in improving thermal conductivity when they are electrically insulating. So, further elaboration is needed in the development of high thermal conductivity polymers with electrical insulation to get the utmost high thermal conductivity in polymer/ceramic composites, since the thermal conductivities of filler ceramics are more likely to depend on their own intrinsic nature and are hardly changed by material science and engineering manipulation.

2.3. LTCC ceramics with high thermal conductivity

Low temperature co-fired ceramics (LTCC) have several benefits in microelectronic packaging. Typical sintering temperature of LTCC is below 1000°C, so they can be co-fired with highly conductive electrodes such as silver (Ag) or copper (Cu) metal. Most of the current LTCC materials are composed of low temperature melting glass matrix and ceramic fillers for functional adjustment such as electrical, mechanical, and thermal properties depending on the requirement of the application. Hence, LTCC is sometimes called glass–ceramics but technically, LTCC is part of glass–ceramic composites. For example, in the field of high frequency (RF, microwave, and mm wave) devices and packaging substrates, low loss and low dielectric constant ceramic powder such as alumina (Al_2O_3) powder is added to the low loss glass matrix. As a result, secondary phases are evolved during the heat treatment process due to part of the alumina filler particles being subjected to react with glass matrix. Interestingly, these secondary phases contribute to the improvement of dielectric properties and mechanical strength when proper filler particle and matrix composition are selected. LTCC has been used for many applications due to energy saving in the low temperature sintering process, excellent dielectric properties,

and ease in 3D integration and miniaturization. Examples are radio frequency-system in-a-package (RF-SiP) module, LED packages, high temperature sensors, microelectromechanical system (MEMS) package, micro-heaters, microfluidics etc. [28–38].

2.3.1. Glass-ceramic base LTCC system

Recently, the use of high thermal conductivity with insulating ceramic substrate is rapidly increasing to enhance the heat transfer property of integrated electronic device and package. Since the conventional LTCCs are based on the glass matrix ceramic composite (GMC) system with low thermal conductivity of the glass phase (1–2 W/mK), the thermal conductivity of most LTCCs are as low as 2–5 W/mK as shown in **Table 6** [38–44], which is still higher than FR-4 (typically 0.1–0.2 W/mK) substrate but far lower than high thermal conductivity bulk ceramics such as alumina, AlN, or Si_3N_4.

Increasing the thermal conductivity in the glass–ceramic system can be realized by recrystallization, addition of high thermal conductivity fillers such as Al_2O_3, AlN, BN, and Si_3N_4 particles.

Category	Maker code/ Chemical composition	Sintering temp (°C)	Thermal conductivity (W/mK)	CTE (ppm/°C)	Dielectric constant	Dielectric loss	Ref.
Commercial products	ESL41110-70C	—	2.5–3	6.4	4.3	0.004	[37, 38]
	Heraeus CT2000	850	3	5.6	9.1	0.002	[37, 39]
	DuPont 951	850	3.2–3.9	5.8	7.8	0.006	[37, 40]
	DuPont 9K7	850	4.6	4.4	7.1	0.001	[37, 41]
	DuPont 943	850	4.4	6	7.4	0.002	[37, 42]
	Ferro A6	850	2	7	5.9	0.002	[37, 43]
	Murata	850	2.5	5.5	7.7	—	[37, 44]
Research works	MgO–CaO–Al_2O_3–SiO_2	900	1.95–2.6	8	—	—	[33, 45]
	$Al2O_3$–BBSZ glass	850	7.2	6.9	10.9	0.009	[46]
	$ZnTiO_3$–B_2O_3	900	6.6	—	20	0.001	[47]
	ABS–MWCNT	—	2.2	—	—	—	[48]
	CAS + β-Si_3N_4	850	7.9	—	7.1	0.006	[49]
	LZT–LMZBS	900	5.8		11.97	—	[50]
	Glass–diamond	750	9.01	4.35	—	—	[51]
	Al_2O_3/glass+ AlN whisker/carbon fiber/ copper fiber	850	38.9	4.6–6.1	6.6–7.4	—	[52]
	Borosilicate glass–AlN–β–Si_3N_4	850	18.8	4.2–4.4	6.5	0.0016	[53]

BBSZ: Bi_2O_3–ZnO–B_2O_3–SiO_2, ABS: Al_2O_3–B_2O_3–SiO_2, CAS: CaO–Al_2O_3–SiO_2, LZT: $Li_2ZnTi_3O_8$, LMZBS: Li_2O–MgO–ZnO–B_2O_3–SiO_2

Table 6. Physical properties of commercial LTCC systems and some of recent research works on high thermal conductivity glass–ceramics.

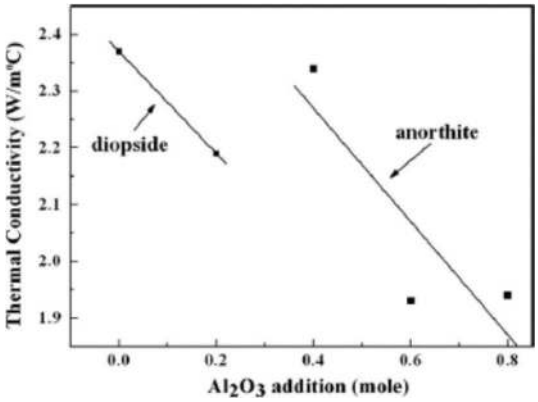

Figure 14. Dependences of thermal conductivity for MgO–CaO–SiO_2–Al_2O_3 glass–ceramic system on Al_2O_3 additions [33, 45].

Various types of filler particle morphologies such as platelet, fibrous types are addressed to improve the inter-particle contact to lower interfacial heat resistance and tailor heat transfer directionality in the substrate. Microstructural manipulations such as filler particle re-orientation, low thermal conductivity, secondary phase removal, and grain boundary control are also explored. Among them, some of key research works are summarized in **Table 6** [33, 45–53].

In the alumina (Al_2O_3) filled glass–ceramic system, MgO–CaO–Al_2O_3–SiO_2, the addition of alumina decreased the thermal conductivity of the glass–ceramic, where diopside or anorthite phase is a major re-crystallized secondary phase as shown in **Figure 14**. The thermal conductivities of diopside-based and anorthite-based glass–ceramics that sintered at <1000°C are 2.37 and 2.35 W/mK, respectively. It was found that the crystallinity is a more important factor than the ratio of dioposide and anorthite such that the highest bending strength and thermal conductivity were obtained at the samples with high crystallinity, since the main peak intensities in the XRD patterns of glass–ceramics is linearly proportional [33, 45]. In the 40 wt% alumina–60 wt% BSSZ (Bi_2O_3–ZnO–B_2O_3–SiO_2) glass system [46], the reported thermal conductivity of 7.2 W/mK is unusually high compared to that of previously known glass–ceramics [38–44] with a high dielectric constant of 10.9 and low loss of 0.009 at the sintered tape.

Aluminoborosilicate (ABS) glass-ceramics containing ≤15 wt% of multiwalled carbon nanotubes (MWCNTs) exhibited an improvement of electrical conductivity by ~10^6 and a thermal conductivity by ~70%. The maximum electrical conductivity of 2.1 S/cm was obtained when 15 wt% MWCNTs was added to an ABS base LTCC, while that of pure ABS was only ~10^{-6} S/cm. The percolation threshold exists at the 2.5–5 wt% MWCNTs added region owing to the uniform dispersion of MWCNTs up to 10 wt%, which is a relatively higher loading rate than others [48] (**Figure 15**).

In the calcium aluminosilicate (CAS) glass system, the thermal conductivity was increased from 1.6 to 7.9 W/mK when 35 vol% of β-Si_3N_4 whiskers added to CAS–Si_3N_4 composites were sintered at 775–850°C in air (**Figure 16)**. This thermal conductivity is much higher than other LTCC systems reported [38–44, 46, 47, 50]. However, the thermal conductivity was decreased when the β-Si_3N_4 whiskers loading exceed 35 wt%. The dielectric constant and loss measured at 1 MHz were 7.1 and 0.006, respectively [49].

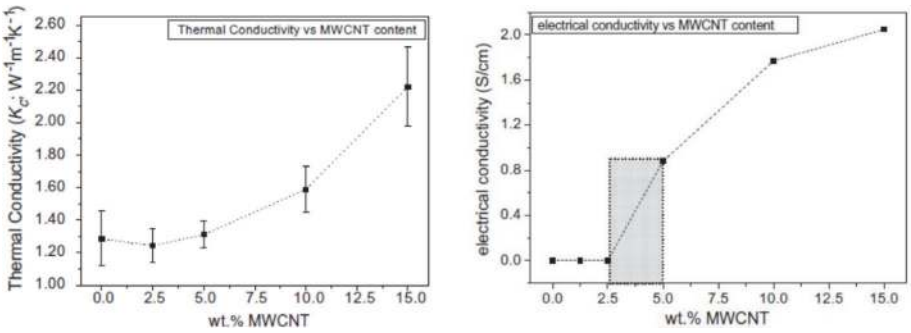

Figure 15. Thermal and electrical conductivity with MWCNT content for the ABS–MWCNT nanocomposites [48].

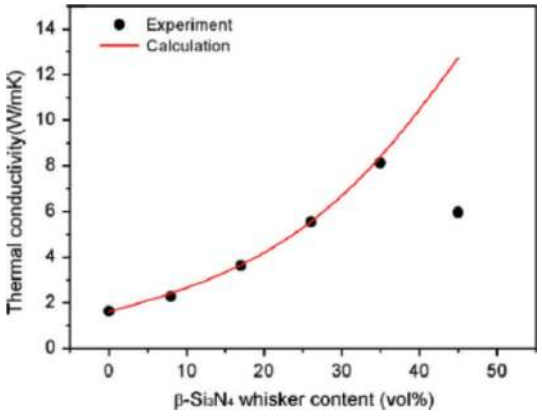

Figure 16. Experimental data and theoretical curve of the thermal conductivity of CAS–Si_3N_4 composites as a function of β-Si_3N_4 whisker contents [49].

The $Li_2ZnTi_3O_8$ (LZT) system with 1 wt% of LMZBS (Li_2O: MgO: ZnO: B_2O_3: SiO_2 = 1: 1: 1: 1: 1) as a sintering aid, thermal conductivity of 5.8 W/mK, and CTE of 11.97 ppm/°C were obtained at samples sintered at 875°C. High dielectric constant and loss of the LZT–LMZBS system at 1 MHz were 24.14 and 5.1 × 10^{-4}, respectively. Microwave dielectric properties of the sintered tape measured by split post dielectric resonator (SPDR) technique were ε_r = 21.9, tan δ = 6 × 10^{-4} at 5 GHz, and τ_ε of −29 ppm/°C [50] (**Figure 17**).

Glass–ceramics filled with 3–40 μm size monocrystal diamond particles were studied, and the results showed highest thermal conductivity at the glass–diamond composites with 30 μm size diamonds that sintered at 750°C and revealed the lowest CTE, the highest thermal conductivity and bending strength: 4.35 ppm/°C, 9.01 W/mK, and 108.25 MPa [51] (**Figure 18**).

The addition of 1D materials such as AlN whiskers, carbon fibers, and copper fibers to the alumina/30 vol% glass composites was studied. The addition of AlN whiskers did not improve the thermal conductivity compared with AlN powder addition and fibrous fillers was more effective in increasing thermal conductivity of the composites. The highest thermal conductivity obtained in these composites was Al_2O_3/glass with 30 vol% copper fibers that sintered at 850°C as shown in

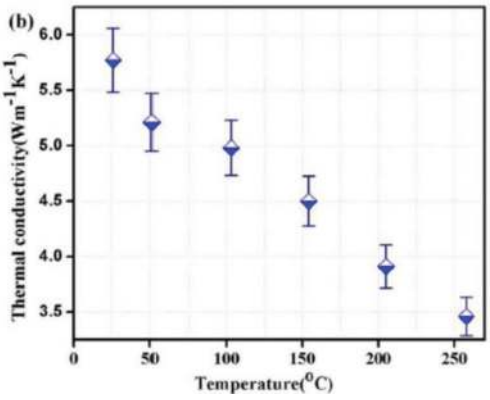

Figure 17. Thermal conductivity measurement data of LZT + LMZBS bulk sintered at 900°C [50].

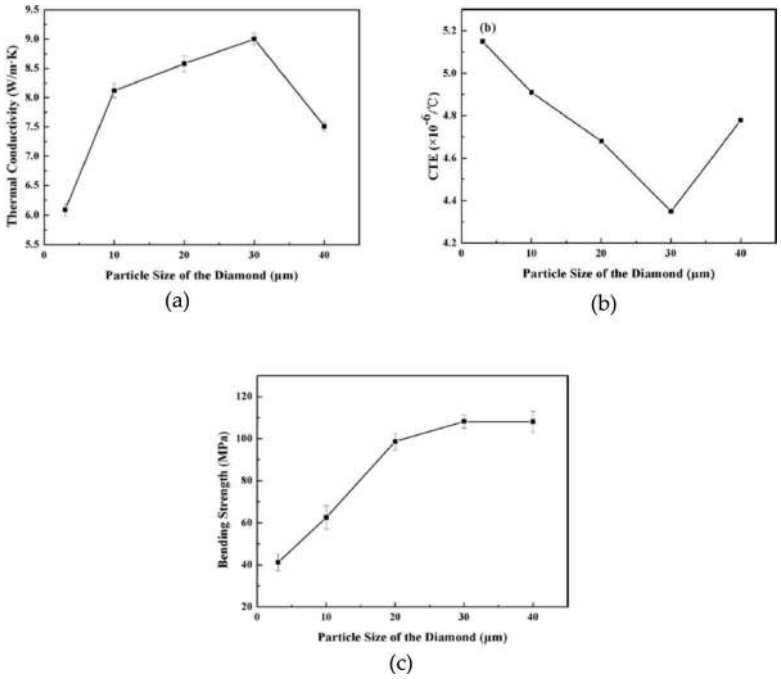

Figure 18. Thermal conductivity (a), CTE (b), and bending strength (c) of glass–diamond LTCCs sintered at 750°C [51].

Figure 19 [52]. The specific resistivity of Al_2O_3/30% glass and Al_2O_3/30% glass/30%AlN-whiskers are 2.0–2.1 × 10^{12} Ω·cm while those of 30% carbon fiber and 30% copper fiber added composites were 8.7 × 10^{-3} and 3.4 × 10^{-6} Ω cm, respectively. Therefore, these two electrically conductive composites are not applicable to electrically insulating thermal management material, or they can be coated with a insulating glass layer on the surface to improve electrical resistivity [52].

In the borosilicate glass–AlN composite LTCC, the thermal conductivity was increased from 11.9 to 18.8 W/mK by the addition of 14 vol% β-Si_3N_4 whiskers as shown in **Figure 20**. This enhanced

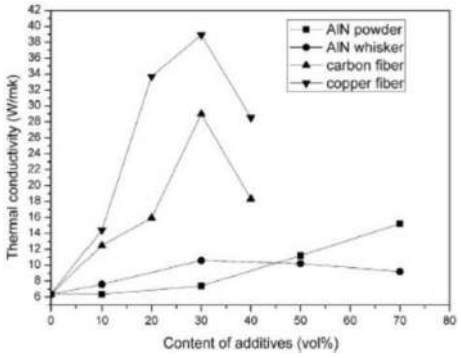

Figure 19. Variation of thermal conductivities of Al_2O_3/glass composites with the addition of 1D filler content [52].

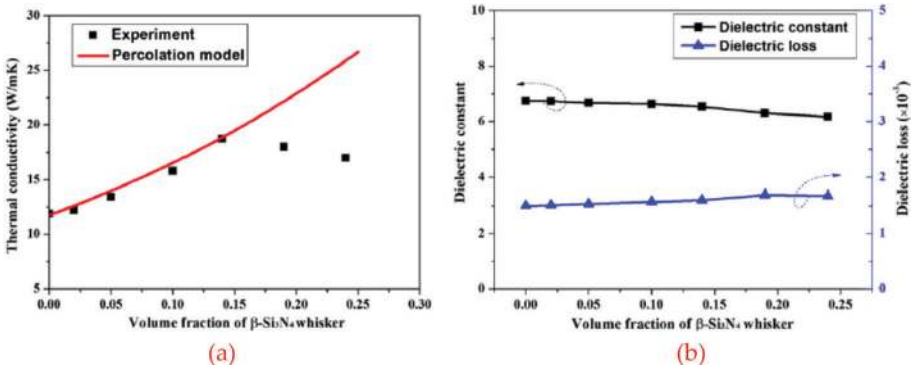

Figure 20. (a) Experimental data and theoretical curve of the thermal conductivity of the CMBS–AlN–Si_3N_4 ceramic composites as a function of β-Si_3N_4 whisker volume fraction and (b) relative dielectric constant and dielectric loss of CMBS–AlN–Si_3N_4 ceramic composites as a function of β-Si_3N_4 whisker volume fraction [53].

thermal conductivity may be due to the formation of a thermal conducting path by bridging the isolated AlN particles through β-Si_3N_4 whiskers. The dielectric properties of this composites are $\varepsilon_r = 6.5$ and $\tan\delta = 0.0016$ at 1 MHz, and the values are not significantly changed with the amount of whiskers due to their similarity in dielectric properties between AlN and Si_3N_4 [53].

2.3.2. Glass-free LTCC system

Glass-free or non-glass base LTCC systems have been investigated to reduce the complexity of the LTCC systems due to the multiple phases included such as glass, filler particles, and additional sintering additives. Due to their complexity, several problems occurred during the preparation of LTCC circuits and devices in the integrated electronic module. To overcome this complexity in chemical interaction and inhomogeneous dielectric properties and difficulties in slurry dispersion, LTCC systems with simple phase components were developed [54–60] (**Table 7**).

In a conventional LTCC system, glass was used as a matrix phase to lower the sintering temperatures below 1000°C because the functional dielectric ceramic materials were mostly fully densified at the high sintering temperatures, over 1200°C, where high electrically conductive

Chemical composition	Sintering temp (°C)	Thermal conductivity (W/mK)	CTE (ppm/°C)	Dielectric constant	tan δ/ Q factor	Reactivity with electrode	Ref.
CaO–(GeO_2, SiO_2, TeO_2)	780–1200	—	—	6.5~19.3	2.4×10^{-3} ~1×10^{-4} (MHz)	N(Ag: germanates, silicate) Y(Ag: tellurate)	[54]
$AMPO_2O_7$ (A = Ca, Sr., M = Zn, Cu)	950	—	—	7.06	52,871 (GHz)	Y(Ag) N(Cu)	[55]
$LiMgPO_4$	950	7.1	10.5	6.4	0.0002	—	[56]
$Bi_4(SiO_4)_3$	900	2.82	7.09	13.3	0.0007 (15GHz)	—	[57]
$Li_2Mg_2Ti_3O_8$	925	—	0.45(τf)	27	58,480 (5.8 GHz)	N(Ag)	[58]
$Li_{2.08}TiO_3$-LiF	900	4.75	22.4	22.4	35,490 (GHz)	N(Ag)	[59]
$11ZnO\text{-}10MoO_3$	850	1.3	4.7	11.1	—	—	[60]

Table 7. Compositions and physical properties of glass-free LTCC systems.

metals such as Ag or Cu cannot be used as a matching electrode. LTCCs containing glass phase matrix generally exhibited low thermal conductivity as we have seen in **Table 6**. In the glass-free LTCCs, lowering the sintering temperature below 1000°C is a primary requirement without introducing secondary phases except the minor content of the sintering agent. Finding a low temperature synthesis and low temperature melting crystalline phase ceramic compound is a crucial point to develop glass-free LTCCs. Glass-free LTCC compositions applicable in the industry with proven mechanical properties and reliabilities are hardly found, even though several primary research results showing excellent dielectric properties were reported [54–60]. The substantial problems exposed in the previous glass-free LTCC systems are weak mechanical strength, reactive with matching electrode materials during heat treatment, and vulnerable in moisture environment.

In the calcium germinates and silicates system, the dielectric constants were 6.5–10.8, quality factor (Q × f) = 16,000–39,000 (@10 GHz), temperature coefficients of dielectric constant were 70–140 ppm/°C for samples sintered at 1180–1200°C, which are slightly higher temperatures for LTCC processing. These systems did not show any chemical reaction with Ag electrode. On the other hand, in the calcium tellurates system, the dielectric constants were 15.5–23.6, Q × f = 13,400–49,300 (~10 GHz), temperature coefficients of dielectric constant were 130–140 ppm/°C for samples sintered at 780–840°C; but this system was vulnerable at Ag electrode. The high temperature coefficients of dielectric constant were suppressed by the addition of 10 mol% of $CaTiO_3$ [54].

For an AMP_2O_7 (A = Ca, Sr.; B = Zn, Cu) system, all of the compounds reacted with Ag but can be co-fired with Cu under reduced atmosphere. Among them, $SrZnP_2O_7$ sintered at 950°C exhibited a dielectric constant of 7.06, Q × f = 52,781 GHz, and temperature coefficient of resonance frequency (τ_f) = −70 ppm/°C; therefore, this compound can be modified into a temperature stable composition if a proper counter dielectric material with negative temperature coefficient is mixed with it. The thermal conductivity of this system was not provided [55].

In the $LiMgPO_4$ tape sintered at 950°C, the microwave dielectric properties were, $\varepsilon_r = 6.4$, tan $\delta = 0.0002$, CTE = 10.5 ppm/°C, and the thermal conductivity was 7.1 W/mK, which is twice as high as that of conventional glass–ceramic base LTCCs. The microwave dielectric properties of sintered tape were measured by using split post dielectric resonator (SPDR) method connected with a vector network analyzer [56].

$Bi_4(SiO_4)_3$ glass-free LTCC tape system has shown dielectric constant of 13.3, loss (tan δ) of 0.0007 at 15GHz, and thermal conductivity of 2.82 W/mK [57]. The $Li_2MgTi_3O_8$ glass-free ceramics sintered at 925°C exhibited a dielectric constant of 27, Q × f value of 58,480 GHz (@5.8 GHz), and very stable temperature coefficient of resonance frequency $\tau_f = 0.45$ ppm/°C. This system is compatible with silver electrode [58]. Another Li-base glass-free LTCC is $Li_{2.08}$ TiO_3–LiF system, where the microwave dielectric properties of $\varepsilon_r = 22.4$, Q × f = 35,490 GHz were obtained at the 900°C sintered tape. The CTE and thermal conductivity of the system were 22.4 ppm/°C and 4.75 W/mK, respectively. The system also is compatible with silver electrode and has a high insulating rate of 50 kV/mm that has a potential in high power application. For the aforementioned glass-free system, the thermal conductivities obtained are 2.28–7.1 W/mK, which is well above that of the most of conventional glass–ceramic base LTCCs [59]. Zinc molybdate with 1% B_2O_3 that sintered at 850–900°C exhibited a dielectric constant of 11.1 CTE of 4.7 ppm/°C, and a break down voltage of 17.6 kV/mm. However, the thermal conductivity was relatively low, 1.4 W/mK, compared to the other glass-free LTCCs. This system may be applicable to high temperature insulating dielectrics due to low CTE and high break down voltage [60].

However, regardless of excellent dielectric and thermal properties, some of the glass-free LTCC compounds containing lithium element have a water soluble problem that limits the application. Therefore, they might need a protective layer coating to resist under weathering conditions.

3. Summary and future prospects

In this chapter, recent research and development works on high thermal conductivity ceramics and their composites for thermal management of integrated electronic packages are briefly explored. Key lessons drawn from these prior works can be summarized as follows:

3.1. High thermal conductivity bulk ceramics

Most frequently found HTCC base high thermal conductivity ceramics are alumina and nitride ceramics such as AlN, BN, and Si_3N_4 materials. Among them, silicon nitride ceramic seems the most frequently used in the power electronic applications these days. In nitrides and nitride based ceramic matrix composites, key parameters that control the thermal property are densification including pore removal, grain size and grain boundary control, impurity, and secondary phase control. Among them, densification is the primary factor to achieve high thermal conductivity due to high thermal resistance of pores. These nitride ceramics are difficult to sinter with high density so that spark plasma sintering and two-step sintering methods together with the addition of small amount of sintering aids should be applied to realize high densification. In nitride ceramics, controlling the oxygen content is a very important factor in addition to the parameters required in oxide materials.

In the LTCC-base materials, there are many research works on the development of high mechanical strength LTCC materials but few works are found in the improvement of thermal conductivity of LTCCs. Some works found in the literature are mainly on re-crystallization and phase control in the matrix and show only minor improvement in thermal properties compared with the noticeable enhancement in mechanical properties. The main reason for this minor change in thermal property in the conventional glass–ceramic type LTCC comes from the glass matrix which comprises more than half the volume of the sintered body. The volume fraction of newly evolved nano-crystalline phases through heat treatment process are so small that the overall apparent thermal conductivity might not change significantly while the mechanical strength can be easily boosted by the inclusion of the nano-crystalline phase in the matrix.

In thermally conductive and electrically conducting ceramics composites, the electrical conductivity was improved with the addition of 2D carbon allotropes like graphene nano sheet/platelet; however, the thermal conductivity was decreased with the involvement of graphene in the AlN matrix, which may be due to the thin interaction layer at the AlN–GNS/GNP interface that would cause thermal resistance. Large difference was observed between the in-plane and through-plane thermal conductivity of the composites as can be observed in the polymer/graphene composites.

3.2. Polymer matrix composites with high thermal conductivity

Polymer matrix composites with high thermal conductivity and electrically insulating ceramic filler materials are mostly used for dielectric insulation layers in LED packaging substrate for effective heat dissipation to the metallic heat spreading panels. Most frequently used insulating ceramic filler materials are alumina, BN, and AlN powders. Among them, BN platelet powders are preferred due to the anisotropic thermal conductivity behavior in the 2D structure of the BN crystal. Lots of researches have been focused on the tailored re-orientation of BN nanosheets in the BN/polymer solution into in-plane or through-plane of the BN/polymer composite tape using magnetic and electric field during casting process. Also, there are some efforts to coat ferrous or dielectric nano particles on BN platelet particles to promote the easy alignment of BN platelet particles into the intended direction. Surface modification of BN particles with functional organics such as silane coupling agent, dopamine, and secondary functional monomers are applied to enhance the thermal conductivity of the composites by improving the BN/polymer affinity and interfacial adhesion, thereby lowering interfacial heat resistance.

Polymer matrix composites with high thermal conductivity inorganic fillers such as CNT, graphite flake, and graphene nanosheets exhibited a great improvement in thermal conductivity with a little amount of additions. However, they are mostly electrically conducting so that they cannot be used for electrical circuit substrates. Instead, these composites are mainly used for thermal interface materials. These polymer/carbon allotropes base composites can also be used for flexible device application as well as rigid substrates since the morphology of carbonates filler particles are 1D or 2D.

3.3. High thermal conductivity ceramics for LED and IGBT packages

Ceramic materials used for applications in LED packages are typically of two types: dielectric insulating substrates for circuit forming bed and high thermal conductivity fillers for thermal

interface material. The insulating ceramic substrates for IGBT modules mostly use alumina, AlN ceramics, but recent development moves to Si_3N_4 and LTCC for high power device due to reliability or low cost.

3.4. Future prospects

Regardless of the aforementioned progresses in the development and commercialization of ceramics, there are several challenges in the high thermal conductivity ceramic based heat transfer materials:

Continuous efforts in lowering costs and cost-effective processing of high temperature sintering HTCCs with high thermal conductivity are required in materials chemistry and innovative processing techniques. Compared to the HTCC based high thermal conductivity ceramics, LTCCs still require further enhancement in both thermal and mechanical characteristics in order to be adopted in thermal management applications. Since the major part of the conventional LTCC formulation consists of glass, the utmost thermal conductivity of the glass–ceramic filler composites thus obtained is limited and far below that of HTCC based high thermal conductivity ceramics. Therefore, first, we need to investigate ways to improve thermal conductivity of the glass phase itself as it is done in many polymer matrix composites. Second, the mechanical strength of LTCC should be further improved even though some results demonstrated enhanced mechanical strength via recrystallization process through the interfacial reaction and nucleation between glass phase and crystalline filler phase. Other challenges in high thermal conductivity LTCCs may be the development of non-glass base LTCCs, which have already been attempted earlier as applications in RF and microwave dielectric materials. The non-glass based LTCCs are exempted from the usage of low thermal conductivity glass matrix phase; they will exhibit higher thermal conductivity than the conventional type.

There are many reports that state the achievement of high thermal conductivities in polymer matrix composites using high thermal conductivity ceramic fillers. As a practical point of view, however, simply increasing thermal conductivity of ceramic filled polymer composites does not ensure the potential use in thermal management application, especially when they are used as thermal interface materials. Other factors, such as adhesion strength to the substrates or heat sink materials for TIM application and tensile strength of thermal tapes or flexible device substrates, also should be considered in addition to thermal and electrical properties since the more filler loading, the less adhesion and tensile strength is provided.

For insulated metal substrates (IMS) using high thermal conductivity ceramics, a reliable solution for CTE mismatch between ceramic and metal joining inducing delamination and crack generation failure in harsh conditions such as cyclic temperature environment is still required. In addition, for highly effective heat transfer performance IMS, we may need an ultra-thin insulation layer with high dielectric breakdown voltage together with high mechanical strength, which enables both low thermal resistance and low package profile of high power device and module.

Acknowledgements

This work was supported by the R&D convergence program of MSIP (Ministry of Science, ICT and Future Planning) and NST (National Research Council of Science & Technology) of the Republic of Korea (Grant No. CAP-13-02-ETRI).

Conflict of interest

None.

Author details

Hyo Tae Kim

Address all correspondence to: hytek@kicet.re.kr

Korea Institute of Ceramic Engineering and Technology, Jinju-si, Gyeongsangnam-do, Republic of Korea

References

[1] Franco Júnior A, Shanafield DJ. Thermal conductivity of polycrystalline aluminum nitride (AlN) ceramics. Cerâmica. 2004;**50**(315). DOI: 10.1590/S0366-69132004000300012

[2] Choi HS, Im HN, Kim YM, Chavan A, Song SJ. Structural, thermal and mechanical properties of aluminum nitride ceramics with CeO_2 as as sintering aid. Ceramics International. 2016;**42**:11519-11524. DOI: 10.1016/j.ceramint.2016.04.028

[3] He X, Yea F, Zhanga H, Liu L. Effect of Sm_2O_3 content on microstructure and thermal conductivity of spark plasma sintered AlN ceramics. Journal of Alloys and Compounds. 2009;**482**:345-348. DOI: 10.1016/j.jallcom.2009.04.013

[4] Kobayashi R, Ohishi K, Tu R, Goto T. Sintering behavior, microstructure, and thermal conductivity of dense AlN ceramics processed by spark plasma sintering with Y_2O_3–CaO–B additives. Ceramics International. 2015;**41**:1897-1901. DOI: 10.1016/j.ceramint.2014.09.040

[5] Lee HM, Kim DK. High-strength AlN ceramics by low-temperature sintering with $CaZrO_3$–Y_2O_3 co-additives. Journal of the European Ceramic Society. 2014;**34**:3627-3633. DOI: 10.1016/j.jeurceramsoc.2014.05.008

[6] Simsek ING, Nistal A, García E, Pérez-Coll D, Miranzo P, Osendi MI. The effect of graphene nanoplatelets on the thermal and electrical properties of aluminum nitride ceramics. Journal of the European Ceramic Society. 2017;**37**:3721-3729. DOI: 10.1016/j.jeurceramsoc.2016.12.044

[7] Yun C, Feng Y, Qiu T, Yang J, Li X, Yu L. Mechanical, electrical and thermal properties of graphene nanosheet/aluminum nitride composites. Ceramics International. 2015;**41**(7):8643-8649. DOI: 10.1016/j.ceramint.2015.03.075

[8] Xia H, Zhang X, Shi Z, Zhao C, Li Y, Wang J. Mechanical and thermal properties of reduced graphene oxide reinforced aluminum nitride ceramic composites. Materials Science and Engineering A. 2015;**639**:29-36. DOI: 10.1016/j.msea.2015.04.091

[9] Liang H, Zengn Y, Zuo K, Xia Y, Yao D, Yin J. Mechanical properties and thermal conductivity of Si_3N_4 ceramics with YF_3 and MgO as sintering additives. Ceramics International. 2016;**42**:15679-15686. DOI: 10.1016/j.ceramint.2016.07.024

[10] Miyazaki H, Yoshizawa Y, Hirao K. Fabrication of high thermal-conductive silicon nitride ceramics with low dielectric loss. Materials Science and Engineering B. 2009;**161**:198-201. DOI: 10.1016/j.mseb.2008.11.029

[11] Golla BR, Ko JW, Kim HD. Processing and characterization of sintered reaction bonded Si_3N_4 ceramics. International Journal of Refractory Metals & Hard Materials. 2017;**68**:75-83. DOI: 10.1016/j.ijrmhm.2017.07.005

[12] Lee HM, Lee EB, Kim DL, Kim DK. Comparative study of oxide and non-oxide additives in high thermal conductive and high strength Si_3N_4 ceramics. Ceramics International. 2016;**42**:17466-17471. DOI: 10.1016/j.ceramint.2016.08.051

[13] Yuan C, Xie B, Huang M, Wu R, Luo X. Thermal conductivity enhancement of platelets aligned composites with volume fraction from 10% to 20%. International Journal of Heat and Mass Transfer. 2016;**94**:20-28. DOI: 10.1016/j.ijheatmasstransfer.2015.11.045

[14] Han Y, Lva S, Haob C, Dinga F, Zhanga Y. Thermal conductivity enhancement of BN/silicone composites cured under electric field: Stacking of shape, thermal conductivity, and particle packing structure anisotropies. Thermochimica Acta. 2012;**529**:68-73. DOI: 10.1016/j.tca.2011.11.029

[15] Cho HB, Nakayama T, Suematsu H, Suzuki T, Jiang W, Niihara K, Song E, Eom NA, Kim S, Choa YH. Insulating polymer nanocomposites with high-thermal-conduction routes via linear densely packed boron nitride nanosheets. Composites Science and Technology. 2016;**129**:205-213. DOI: 10.1016/j.compscitech.2016.04.033

[16] Zhang J, Wang X, Yu C, Li Q, Li Z, Li C, Lu H, Zhang Q, Zhao J, Hu M, Yao Y. A facile method to prepare flexible boron nitride/poly(vinyl alcohol) composites with enhanced thermal conductivity. Composites Science and Technology. 2017;**149**:41-47. DOI: 10.1016/j.compscitech.2017.06.008

[17] He X, Gong Q, Guo Y, Liu J. Microstructure and properties of AlN-BN composites prepared by sparking plasma sintering method. Journal of Alloys and Compounds. 2016;**675**:168-173. DOI: 10.1016/j.jallcom.2016.03.058

[18] Li YL, Zhang J, Zhang JX. Fabrication and thermal conductivity of AlN/BN ceramics by spark plasma sintering. Ceramics International. 2009;**35**:2219-2224. DOI: 10 .1016/j.ceramint.2008.12.003

[19] Zhao H, Wang W, Fu Z, Wang H. Thermal conductivity and dielectric property of hot-pressing sintered AlN–BN ceramic composites. Ceramics International. 2009;**35**:105-109. DOI: 10.1016/j.ceramint.2007.09.111

[20] Wilk A, Rutkowski P, Zientara D, Bu'cko MM. Aluminium oxynitride–hexagonal boron nitride composites with anisotropic properties. Journal of the European Ceramic Society. 2016;**36**:2087-2092. DOI: 10.1016/j.jeurceramsoc.2016.02.029

[21] Kim K, Ju H, Kim J. Filler orientation of boron nitride composite via external electric field for thermal conductivity enhancement. Ceramics International. 2016;**42**:8657-8663. DOI: 10.1016/j.ceramint.2016.02.098

[22] Zhan Y, Long Z, Wan X, Zhan C, Zhang J, He Y. Enhanced dielectric permittivity and thermal conductivity of hexagonal boron nitride/poly(arylene ether nitrile) composites through magnetic alignment and mussel inspired co-modification. Ceramics International. 2017;**43**:12109-12119. DOI: 10.1016/j.ceramint.2017.06.068

[23] Jang I, Shin KH, Yang I, Kim H, Kim J, Kim WH, Jeon SW, Kim JP. Enhancement of thermal conductivity of BN/epoxy compositethrough surface modification with silane coupling agents. Colloids and Surfaces A: Physicochemical and Engineering Aspects. 2017;**518**:64-72. DOI: 10.1016/j.colsurfa.2017.01.011

[24] Lee ST, Kim HT, Nahm S, Lee SH, Lee SG. Fabrication of high thermal conductivity ceramic hybrid meatrials for power electronics and integrated packages. In: Proceedings of HEFAT; 20-23 July 2015

[25] Zhou Y, Wang H, Wang L, Yu K, Lin Z, He L, Bai Y. Fabrication and characterization of aluminum nitride polymer matrix composites with high thermal conductivity and low dielectric constant for electronic packaging. Materials Science and Engineering B. 2012;**177**:892-896. DOI: 10.1016/j.mseb.2012.03.056

[26] Hu M, Feng J, Ng KM. Thermally conductive PP/AlN composites with a 3-D segregated structure. Composites Science and Technology. 2015;**110**:26-34. DOI: 10.1016/j.compscitech.2015.01.019

[27] Wozniak M, Anna Danelska A, Rutkowski P, Kata D. Thermal conductivity of highly loaded aluminium nitride–poly(propylene glycol) dispersions. International Journal of Heat and Mass Transfer. 2013;**65**:592-598. DOI: 10.1016/j.ijheatmasstransfer.2013.06.048

[28] Chen C, Hou F, Liu F, She Q, Cao L, Wan L. Thermo-mechanical reliability analysis of a RF SiP module based on LTCC substrate. Microelectronics Reliability. 2017;**79**:38-47. DOI: 10.1016/j.microrel.2017.10.003

[29] Nowak D, Dziedzic A. LTCC package for high temperature applications. Microelectronics Reliability. 2011;**51**:1241-1244

[30] Chutani RK, Galliou S, Passilly N, Gorecki C, Sitomaniemi A, Heikkinen M, Kautio K, Keranen A, Jorno A. Thermal management of fully LTCC-packaged Cs vapour cell for MEMS atomic clock. Sensors and Actuators A. 2012;**174**:58-68

[31] Jiang B, Muralt P, Maeder T. Meso-scale ceramic hotplates – A playground for high temperature microsystems. Sensors and Actuators B. 2015;**221**:823-834

[32] Vasudev A, Kaushik A, Tomizawa Y, Norena N, Bhansali S. An LTCC-based microfluidic system for label-free, electrochemical detection of cortisol. Sensors and Actuators B. 2013;**182**:139-146. DOI: 10.1016/j.snb.2013.02.096

[33] Kang M, Kang S. Influence of Al_2O_3 additions on the crystallization mechanism and properties of diopside/anorthite hybrid glass-ceramics for LED packaging materials. Journal of Crystal Growth. 2011;**326**:124-127. DOI: 10.106/j.jcrysgro.2011.01.081

[34] Liu S, Li X, Yu X, Chang Z, Che P, Zhou J. A route for white LED package using luminescent low-temperature co-fired ceramics. The Journal of Alloys and Compounds. 2016;**655**:203-207. DOI: 10.1016/j.jallcom.2015.09.177

[35] Ding Y, Liu YS, Li X, Wang R, Zhou J. Luminescent low temperature co-fired ceramics for high power LED package. The Journal of Alloys and Compounds. 2012;**521**:35-38. DOI: 10.1016/j.jallcom.2011.12.143

[36] Bienert C, Roosen A. Characterization and improvement of LTCC composite materials for application at elevated temperatures. Journal of the European Ceramic Society. 2010;**30**:369-374. DOI: 10.1016/j.jeurceramsoc.2009.05.023

[37] Sebastian MT, Jantunen H. Low loss dielectric materials for LTCC applications: A review. International Materials Reviews. 2018;**53**:57-90. DOI: 10.1179/174328008X277524

[38] Golonka LJ. Technology and applications of low temperature co-fired ceramic (LTCC) based sensors and microsystems. Bulletin of the Polish Academy of Sciences, Technical Sciences. 2006;**54**:221-231

[39] http://natelems.com/wp-content/uploads/2014/10/Natel-LTCC-Quick Ref.pdf. Heratape™ CT2000

[40] http://www.dupont.com, DataSheetofDupontTM Green TapeTM 951

[41] http://www.dupont.com, DataSheetofDupontTM Green TapeTM 9K7

[42] http://www.ltcc-consulting.com/LTCC_technology_materials

[43] http://www.dupont.com/content/dam/assets/products-and-services/electronic-electrical materials/ assets/datasheets/prodlib/943LowLossTape.pdf

[44] http://www.murata.com-Murata's LTCCsubstratetechnology: LFC Series

[45] Jang S, Kang S. Influence of MgO/CaO ratio on the properties of MgO–CaO–Al_2O_3–SiO_2 glass–ceramics for LED packages. Ceramics International. 2012;**38S**:S543-S546. DOI: 10.1016/j.ceramint.2011.05.073

[46] Induja IJ, Abhilash P, Arun S, Surendran KP, Sebastian MT. LTCC tapes based on Al_2O_3–BBSZ glass with improved thermal conductivity. Ceramics International. 2015;**41**:13572-13581. DOI: 10.1016/j.ceramint.2015.07.152

[47] Kim HT, Kim SH, Nahm S, Byun JD. Low-temperature sintering and microwave dielectric propertiesof zinc metatitanate-rutile mixtures using boron. The Journal of the American Ceramic Society. 1999;**82**(11):3043-3048. DOI: 10.1111/j.1151-2916.1999.tb02200.x

[48] Mukhopadhyay A, Otieno G, Chu BTT, Wallwork A, Green MLH, Todd RI. Thermal and electrical properties of aluminoborosilicate glass–ceramics containing multiwalled carbon nanotubes. Scripta Materialia. 2011;**65**:408-411. DOI: 10.1016/j.scriptamat.2011.05.023

[49] Ma M, Liu Z, Li Y, Zeng Y, Yao D. Thermal conductivity of low-temperature sintered calcium aluminosilicate glass–silicon nitride whisker composites. Ceramics International. 2013;**39**:4683-4687. DOI: 10.1016/j.ceramint.2012.11.056

[50] Arun S, Sebastian MT, Surendran KP. $Li_2ZnTi_3O_8$ based high κ LTCC tapes for improved thermal management in hybrid circuit applications. Ceramics International. 2017;**43**:5509-5516. DOI: 10.106/j.ceramint.2017.01.073

[51] Feng D, Li Z, Zhu Y, Ji H. Influence of diamond particle size on the thermal and mechanical properties of glass-diamond composites. Materials Science and Engineering B. 2018;**227**:122-128. DOI: 10.1016/j.mseb.2017.10.017

[52] Wang S, Zhang D, Ouyang X, Wang Y, Liu G. Effect of one-dimensional materials on the thermal conductivity of Al_2O_3/glass composite. Journal of Alloys and Compounds. 2016;**667**:23-28. DOI: 10.1016/j.jallcom.2016.01.120

[53] Ma M, Liu Z, Li Y, Zeng Y, Yao D. Enhanced thermal conductivity of low-temperature sintered borosilicate glass–AlN composites with β-Si_3N_4 whiskers. Journal of the European Ceramic Society. 2013;**33**:833-839. DOI: 10.1016/j.jeurceramsoc.2012.09.030

[54] Valant M, Suvorov D. Glass-free low-temperature cofired ceramics: Calcium germanates, silicates and tellurates. Journal of the European Ceramic Society. 2004;**24**:1715-1719. DOI: 10.1016/S0955-2219(03)00483-7

[55] Bian JJ, Kim DW, Hong KS. Glass-free LTCC microwave dielectric ceramics. Materials Research Bulletin. 2005;**40**:2120-2129. DOI: 10.1016/j. materresbull.2005.07.003

[56] Thomas D, Abhilash P, Sebastian MT. Casting and characterization of $LiMgPO_4$ glass free LTCC tape for microwave applications. Journal of the European Ceramic Society. 2013;**33**:87-93. DOI: 10.1016/j.jeurceramsoc.2012.08.002

[57] Abhilash P, Sebastian MT, Surendran KP. Glass free, non-aqueous LTCC tapes of $Bi_4(SiO_4)_3$ with high solid loading. Journal of the European Ceramic Society. 2015;**35**:2313-2320. DOI: 10.106/j.jeurceramsoc.2015.02.002

[58] Zhou H, Wang N, Gong J, Fan G, Chen X. Processing of low-fired glass-free $Li_2MgTi_3O_8$ microwave dielectric ceramics. Journal of Alloys and Compounds. 2016;**688**:8-13. DOI: 10.1016/j.jallcom.2016.07.214

[59] Bian JJ, Yu Q, He JJ. Tape casting and characterization of $Li_{2.08}TiO_3$-LiF glass free LTCC for microwave applications. Journal of the European Ceramic Society. 2017;**37**:647-653. DOI: 10.1016/j.jeurceramsoc.2016.09.022

[60] Wang Z, Freer R. Low firing temperature zinc molybdate ceramics for dielectric and insulation applications. Journal of the European Ceramic Society. 2015;**35**:3033-3042. DOI: 10.1016/j.jeurceramsoc.2015.04.020